„*Caius Iacob*" **Conference on**
Fluid Mechanics&Technical Applications
Bucharest, Romania, November 2005

Higher resolution Thermal design of an HTS AC armature winding

by
Alexandru Mihail Morega[1], Juan Carlos Ordonez[2], Petrica Andrei Negoias[1]

[1]Department of Electrical Engineering
POLITEHNICA University of Bucharest, Bucharest 060042, Romania
[2]Department of Mechanical Engineering and Center for Advanced Power Systems
Florida State University, Tallahassee, FL 32310

ABSTRACT

This paper reports a numerical heat transfer study, which is part of our efforts devoted to defining a cooling concept for a high performance synchronous motor that has a High Temperature Superconductor (HTS) field winding. Whereas the rotor of this machine is the HTS DC field winding, the armature is a high current AC copper "air winding" that is siege of intense power dissipation by Joule and variable magnetic field effects. Consequently, prototyping a low weight/volume motor results in a complex thermal design where an important role is played by the thermal management of the AC winding.

Standard lumped thermal circuit models deliver fast, design class results that reveal the heat transfer underlying features. However, there are several difficulties related to this approach consistent with the specific assumptions (e.g., concentrated heat sources, lack of detailed thermal load information, etc.) that may be solved by a more detailed convection and conduction heat transfer model, conveniently solved by numerical analysis, e.g. by FEM technique.

1. INTRODUCTION

The high performance synchronous motor with High Temperature Superconductor (HTS) field winding is a promising technology for both naval and next generation airborne applications. Prototyping a low weight/volume HTS motor leads inevitably to dedicated thermal design that may exceed the level of detail requested by standard electrical machines [1], [2]: in particular, the armature of an HTS motor is usually an AC copper winding, also called "air-winding", which is mounted in an iron-less stator. This unconventional winding is siege of intense power dissipation by Joule and variable magnetic field effects, and has to be thoroughly designed to provide for the thermal stability of the HTS motor.

The standard thermal design procedure consists of drawing the equivalent thermal lumped circuit model [3]-[5]. This approach is still most convenient for a first stage accurate analysis: it provides for a general overview of the temperature field within the structure, and permits also a direct and relatively simple integration with the electromagnetic design [6]-[8].

However, as with all lumped models, there are intrinsic limitations – e.g., the heat sources are assumed concentrated rather than distributed, the temperature field is estimated in a few number of points – that may not be easily circumvented when more detailed information is needed. For in-depth knowledge of the thermal field beyond the information delivered by the lumped circuit model [9], and in order to evaluate the quality of the design we investigated numerically the steady state heat transfer problem (energy equation, momentum and mass conservation laws) with FEMLAB [10]. First, a simplified 2D axial-symmetric model is formulated: it accounts for the steady state forced convection heat transfer within the motor. Next, a FEM analysis of detailed 3D model aimed at investigating the enthalpy paths in a critical part of the stator is presented.

2. PHYSICAL AND MATHEMATICAL MODELS

The stator–rotor ensemble is a cylindrical structure made of coaxial layers with anisotropic heat transfer properties (Fig.1): heat is well transferred axially and constrained in the radial direction, where higher temperature drops are likely to exist.
The electromagnetic shield that confines the rotor is acting as a thermostat, which – from the stator point of view – receives heat by forced convection, turbulent Taylor-Couette flow [5], through the rotor-stator air gap. The stator case generates heat, receives heat, and conveys it through three mechanism [6]: conduction through the air-gap that separates the case from the armature, conduction from the end parts of the winding, and natural convection through the path end winding – inside air – case.

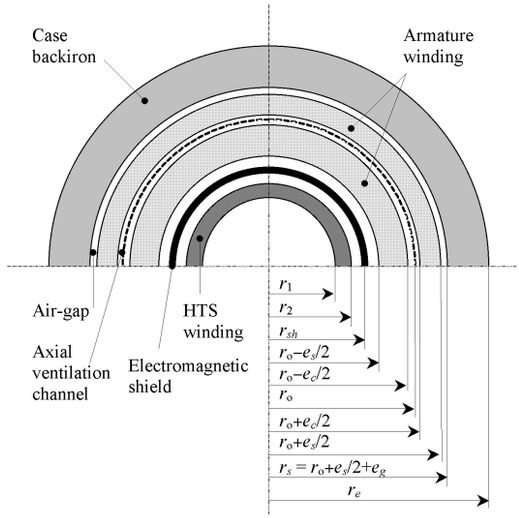

Fig. 1 Cross sectional view of the HTS motor [9].

The armature winding is made of impregnated, insulated Litz copper wires. This structure is thermally anisotropic and may be characterized by different radial and axial thermal conductivities: in axial direction the copper wires, insulation and impregnation layers conduct the heat current in parallel, whereas in radial direction they conduct heat mainly in series [5].
Since the heat generated within the armature winding is indirectly evacuated (after crossing through different parts of the machine) and since the thermal load is high, we propose an armature winding packaging that is provided with a supplementary, coaxial annular channel within it, centered about r_o (Fig.2).

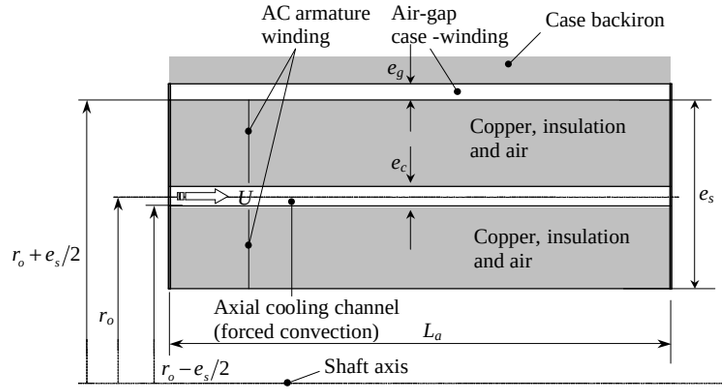

Fig.2 The armature winding and the internal forced convection cooling channel.

This axial channel cooled by laminar forced convection separates the winding into two cylindrical concentric parts, providing for a direct heat path; for a closed machine, it delivers the heat drained out from the winding to the end parts of the machine, where it is discarded at the inside air temperature.
At this stage, we are interested in the steady-state regime of the motor therefore the thermal inertia that is important for transient regime analysis is not considered.

3. THE 2D AXIAL MODEL – RESULTS AND DISCUSSION

The axial symmetry of rotating machines suggests that a 2D axial model may satisfactorily represent the actual airflow and temperature fields in the real 3D object. The following assumptions make the framework for the analysis:

- The rotating machine has axial symmetry; each cylindrical layer (winding, case, etc.) is geometrically and thermally symmetric in azimuth direction.
- The machine is totally closed, forced convection cooled (TEFC);
- The heat sources (Joule effect by conduction and eddy currents, hysteretic losses) are uniformly distributed in the active parts of the stator (copper winding and iron case);
- Radiation heat transfer to the ambient is not accounted for – its contribution is assumed small as compared to convection and conduction processes, whereas its strong non-linear nature would introduce computational difficulties;
- The stator is thermally decoupled from the HTS rotor, whose outer surface (the electromagnetic shield) is at the inside temperature of the machine;
- The iron case, the air in the cooling channel and within the air gap between the armature winding and the case are assumed isotropic, homogeneous, linear media;
- Due to the composite nature of the armature winding (insulated, impregnated Litz copper wire and air trapped in-between), we found it important to consider this domain as linear, homogeneous but anisotropic, with different thermal conductivities in axial and radial directions, eq. (3).
- The facing faces the stator armature and rotor damper are assumed cylindrical, concentric, smooth. Consequently, no saliency or surface roughness-related effects that may influence the airflow within the air-gap are present.

Heat transfer within the stator is by conduction, and it is governed by the energy equation

$$\nabla \cdot \left(\bar{\bar{k}} \nabla T\right) + q_o = 0, \tag{1}$$

where q_o is the heat source (W/m^3) – Joule losses in the armature winding and AC losses in the iron case – and $\bar{\bar{k}}$ is thermal conductivity tensor [11], [12].
The cooling axial channel inside the winding is siege of a stationary, incompressible, laminar forced airflow, characterized by the momentum and mass conservation laws [11], [12]

$$\rho(\mathbf{u} \cdot \nabla) \cdot \mathbf{u} = -\nabla p + \mu \nabla^2 \mathbf{u}, \tag{2}$$

$$\nabla \mathbf{u} = 0. \tag{3}$$

Heat transfer here is by forced convection, without internal heat generation

$$\rho c_p (\mathbf{u} \cdot \nabla) T = \nabla \cdot \left(\bar{\bar{k}} \nabla T\right). \tag{4}$$

The properties that intervene (mass density, ρ, dynamic viscosity of the coolant, μ, thermal conductivity, $\bar{\bar{k}}$, specific heat, c_p) are assumed constant, evaluated at the average, working temperature of the motor.

As the machine under investigation is of TEFC type, an important parameter is the inside air temperature, T_i. We assume that the internal convection heat transfer (e.g., end winding to inside air) is with respect to the inside temperature – set here at 50°C. The inlet temperature of the cooling air (the channel within the armature winding) is T_{amb} = 30°C. Also, heat transfer at the outlet is by convection only. The computational domain and the boundary conditions are shown in Fig.3*a*,*b*.

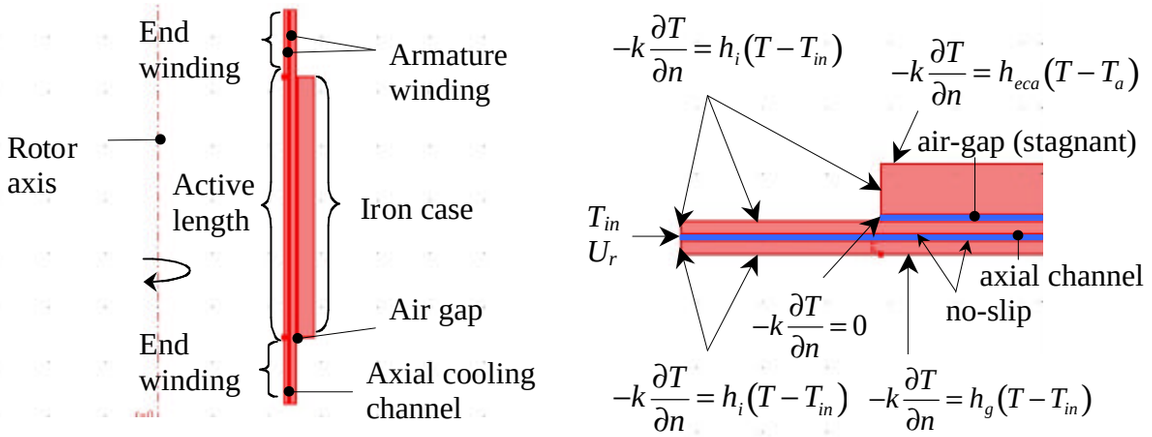

a. 2D axial model of the AC stator. **b**. Boundary conditions for the heat transfer problem.

Fig.3 Computational domain (a) and boundary conditions for the temperature field (b) – FEMLAB model.

The inlet velocity profile is assumed axial, uniform, at 5 m/s. The convection heat transfer coefficients are h_{eca} = 40 W/m^{2}K, h_i = 80W/m^{2}K, h_g = 10 W/m^{2}K. The total axial length is 363 mm, the active length (equal to the case axial length) is 240 mm, the armature winding is a cylindrical shell 10.5 mm thick, the axial cooling channel inside the winding is a cylindrical shell 2 mm wide (in radial direction), the case is a cylindrical shell 16 mm thick.

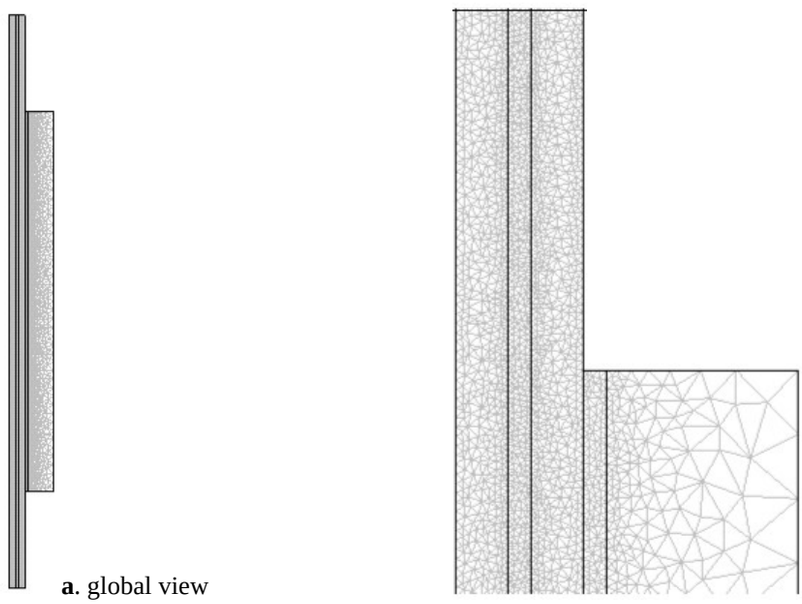

a. global view **b**. detail

Fig.4 the FEM mesh – Delauney, unstructured mesh with P_1-P_2 Lagrange elements (~29000 elements)

The 2D axial model numerically solved by the FEM Galerkin scheme, as implemented by FEMLAB [10]. Figure 4 shows the discretization mesh made of roughly 29000 Langrange elements (P_2-P_3 for flow, and quadratic for temperature) that provides for grid-independent solutions.

As in forced convection the heat transfer the flow part of the problem is decoupled from the energy equation, we first solved for the flow field and then, using the velocity field thus obtained, we integrated for the temperature field – this strategy, used in forced convection problems, greatly reduces the computational effort and time without loss of accuracy.

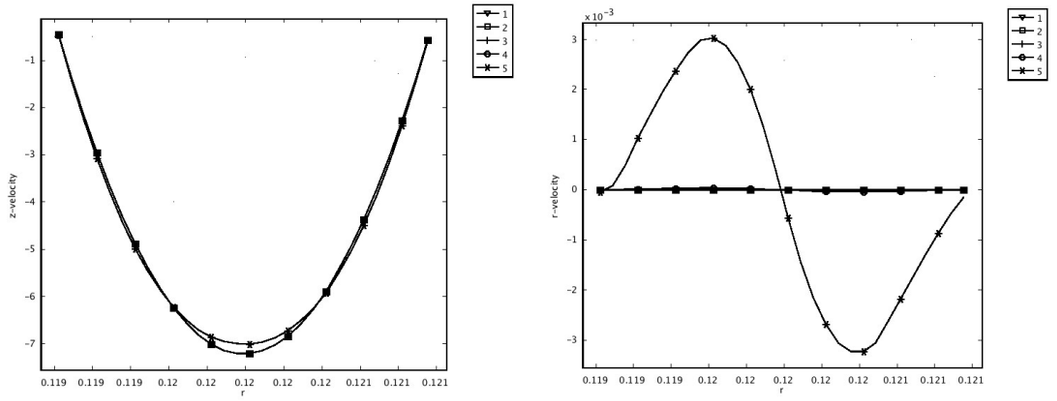

Fig.5 Velocity profile at five different locations indication the fully developed nature of the flow.

Figure 5 shows the velocity profiles at five, uniformly distributed cross-sectional locations. Apparently the resulting flow is as expected Hagen-Poiseuille, fully developed over almost its entire length [9].

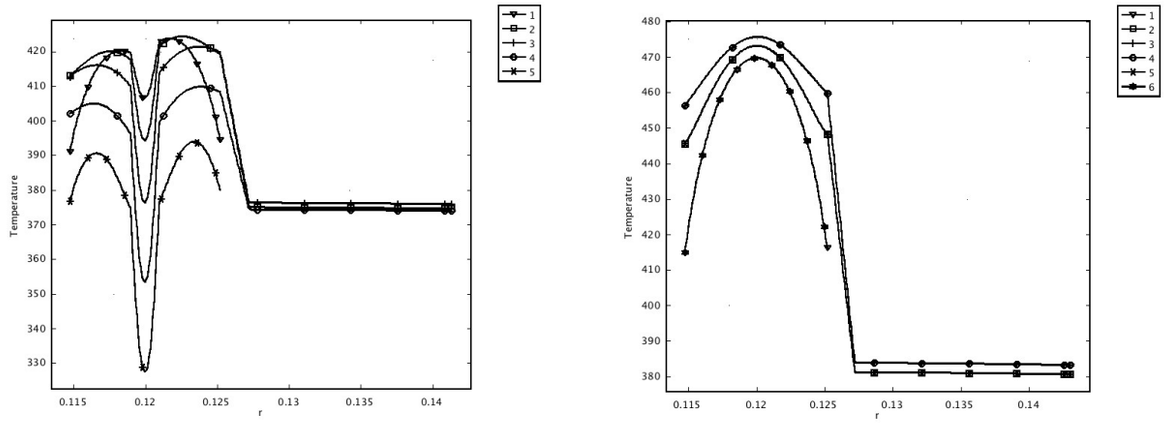

a – with axial cooling channel. **b** – without the cooling channel.

Fig.6 The temperature profile at five different cross-sectional locations.

An important temperature drop occurs at the channel's level (Fig.6). *The role played by this cooling mean is important to the thermal management of the armature winding, reducing the high spot temperature and the temperature drops* (gradients) – compare the graphs in Fig.8,*a* and Fig.8,*b* that show a reduction of approx. 50°C in the highest temperature provided by the design that utilizes the axial cooling channel. Figure 8,*b* confirms the expected symmetry of the temperature field with respect to the middle radial cross-section.

In both situations, the iron case is almost isothermal. The air gap between the armature winding and the iron case produces a large temperature drop. Alternatively, this effect may be modeled through a thermal contact resistance [13] that replaces the actual gap.
The trail region of the armature winding (in stream-wise direction) registers the highest temperatures. If the coolant is air, for the inlet speed of 9 m/s ($\mathrm{Re}_{D_h} = 2193$) and the inlet temperature of 50°C, the outlet reaches ~80°C, whereas the hot spot temperature within the stator is below 110°C. For *N* (e.g., Kaptan FCR group), *H* or *F*-class insulations these values are acceptable [14]. Next, a detailed 3D thermal analysis concerning a part of the AC winding is considered.

4. THE 3D MODEL – RESULTS AND DISCUSSION

The purpose of this study is to assess the effectiveness of axial cooling channels, and to promote their usage in the thermal management of HTS AC armature winding. We are concerned with finding the fine details of the heat transfer process not unveiled by the lumped circuit scheme and 2D axial FEM models. The optimization of the thermal design makes the object of future research. Here, we were concerned with the effect of axial cooling channel inside the winding, and with the role of the air-gap between stator and winding. As the numerical simulation of the entire machine is still beyond commonly available computing resources, we focus on a particular region that is likely to be less accurately modeled by lumped circuit and 2D axial FEM models. We report the numerical results obtained by FEM analysis for critical region of this ensemble.
Figure 7 shows a qualitative cross-sectional view of the armature winding. First, we assume that the case-winding air gap confines trapped air, and model it as a thermal contact resistance. The case when the air gap is large enough to be used as a secondary axial cooling channel is not reported here. The computational domain is defined with satisfactorily accuracy by assuming that the stator ensemble presents geometric periodicity as consequence of the relatively regular structure of the consolidation skeleton (epoxy spacers).

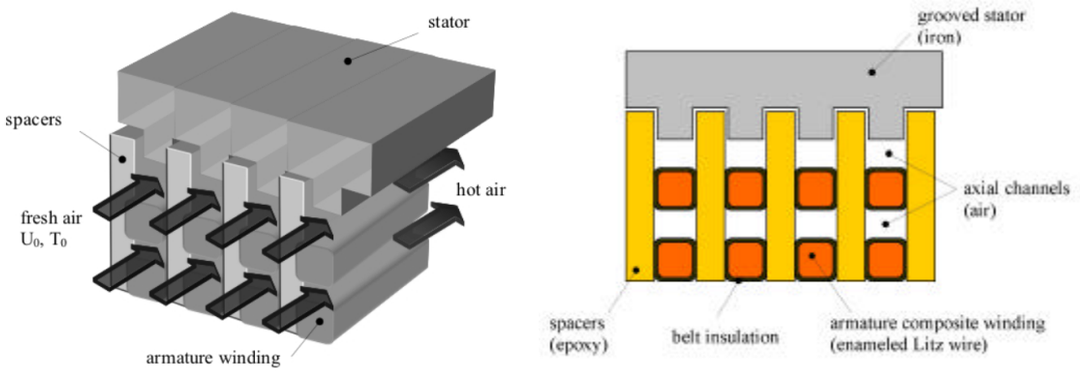

a. Axonometric view **b.** Cross-sectional view

Fig.7 The armature air-winding – qualitative views

The mathematical model consists of eqs. (1) – (4), added with adequate boundary conditions for the region cut-off for investigation.
Figure 8 shows the FEM model for the air-gap replaced by a thermal contact interface. This approach is consistent with negligible small winding to case gap. The model reported here considers only three spacers, whereas in the actual machine there may be more. This is a simplification made to reduce the complexity of the numerical model.

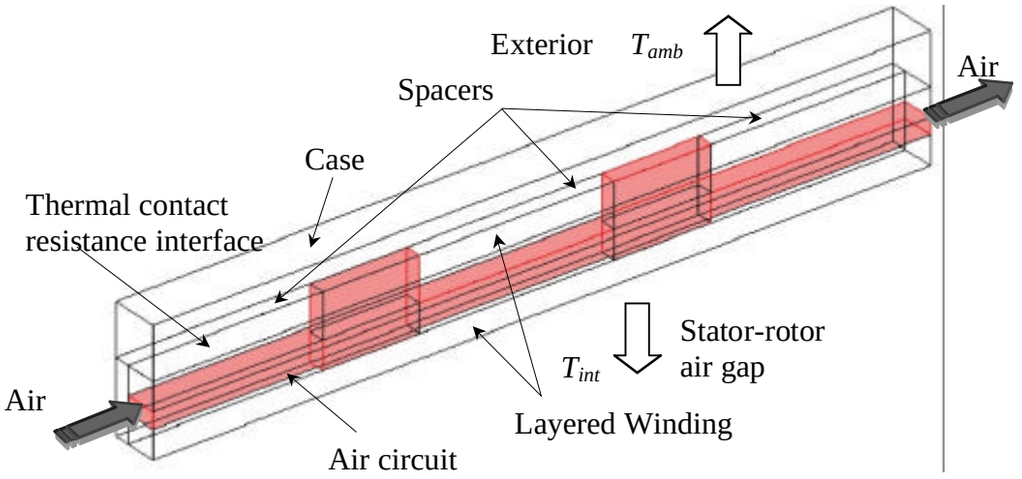

Fig.8 Thermal contact model – the air circuit is marked in red.

First the flow part of the problem (2), (3) is solved for the air circuit domain. We assume no-slip velocity boundary conditions at the solid walls, slip/symmetry velocity boundary conditions on the symmetry planes *xOz*, uniform velocity profile at the inlet and constant pressure profile at the outlet.

The heat transfer problem is solved then for the entire structure: conduction within the solid regions (winding, case, spacers) and forced convection within the air circuit domain. To model the case to winding air gap as a thermal contact interface in FEMLAB environment we divided the heat transfer problem into two parts (regions): the case (one problem) and the rest of the structure (the second problem). For these two problems the case-winding gap/interface becomes boundary. The specific conditions – basically, heat flux conservation – are explained in Fig.9. The contact thermal conductivity of the interface, h_i, (here, 540 W/m^{2}K) is an empiric quantity evaluated following the guidelines outlined in [13].

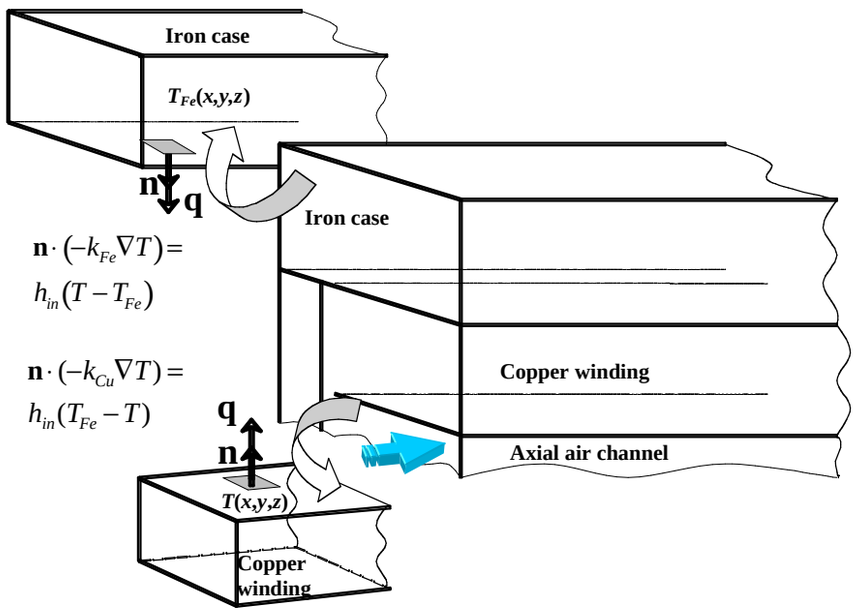

Fig. 9 The interface thermal conductance model

The stator to rotor convection heat flux coupling through the air gap is accounted for through a heat transfer coefficient 10 W/m^{2}K. The cavities between the epoxy spacers and the armature

winding do not communicate with the stator to rotor air gap. These hypotheses lead to a temperature field that slightly overestimates the stator thermal load, acceptable to a "safe-limit" class design. Heat transfer from the stator to the ambient is by natural convection, with a heat transfer coefficient of 5 W/m^2K. All other surfaces (including the axial channel outlet) are assumed adiabatic.

The following strategy is used to solve this forced convection heat transfer problem: first, the flow part is solved; the two heat transfer problems are solved then simultaneously providing for the temperature and heat flux with the entire structure.

Figure 10 depicts the numerical results through isotherm profiles at the entrance and exit sections of the axial cooling channel. The inlet velocity is 0.8 m/s – approximately beyond this limit the flow becomes unstable.

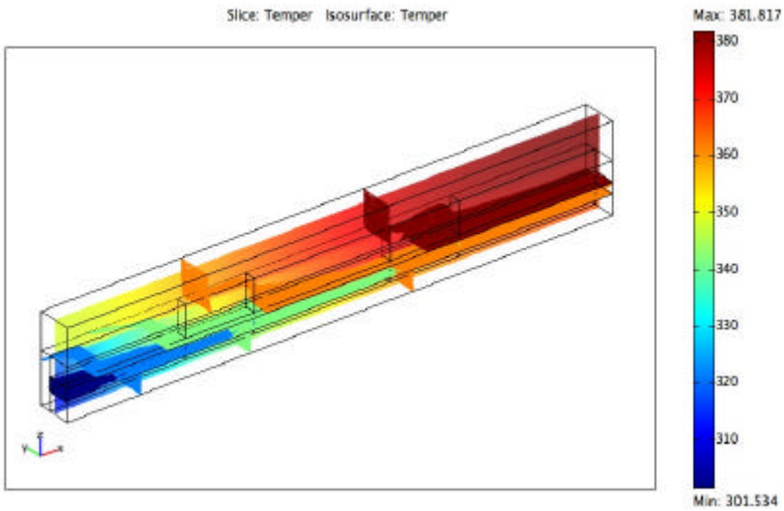

a. Temperature slice and isotherms.

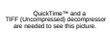

b. Upstream section. **c.** Downstream section.

Fig. 10 Heat transfer in the stator of the HTS machine.

The shape and structure of the isotherms express the different heat transfer mechanisms within the structure and it is remarkably complex. From case to winding, the isotherms profiles change in shape and slope: they are almost vertical in the stator case (thermal conduction in a good thermal conducting medium), then a large jump (a $\pi/2$ bent) at the case-winding thermal contact interface, another almost vertical profile in the upper part of the winding (conduction in a good thermal conducting medium), a complex profile in the channel (forced convection), and again an almost vertical profile (conduction) within the lower half of the winding. If air gap spacing is not that small or this region is intended to work as a secondary cooling channel the thermal contact resistance model may no longer be accurate.

Figure 11 details the flow structure and thermal load within the two passages connected to the axial channel. The color of the streamlines is proportional to the local temperature. The arrows

(velocity) are normalized (i.e., they have the same module) to better evidence the flow and heat current details.

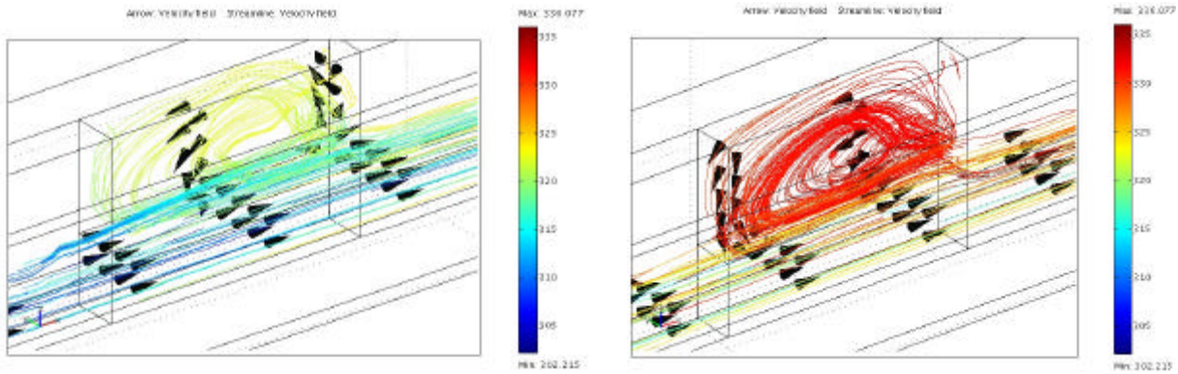

a. The upstream passage. **b.** The downstream passage.

Fig. 11 Flow structure and thermal load details – note the separation interfaces suggested by the streamlines.

The air trapped within the passage windows is much warmer than the air in the axial channel, and the downstream cavity traps warmer air then its upstream neighbor. Heat transfer between the secondary, cavity flows and the main stream is by diffusion across the separation interfaces. Apparently the highest temperature (~110ºC) is within safe, design limits provided high quality thermal insulations is used.

5. CONCLUSIONS

Thermal management, a key issue in prototyping electrical machines, poses non-trivial problems in the design of HTS synchronous machines for both the rotor (the HTS armature) and the stator (the AC, air-winding armature). Specifically for the stator much larger than usual current loads are packed in the stator AC air winding. Consequently, the heat to be dissipated per unit of stator external surface is much larger than for conventional machines. Therefore unconventional design solutions are required to keep the thermal load within safe, design limits. The axial channel proposed here provides for the supplementary enthalpy drain that reduces the maximum temperature below the acceptable threshold.

In this paper we present two FEM approaches to the numerical evaluation of this design receipt. The first, 2D axial model gives satisfactorily accurate results, but does not evidence the fine details of the thermal picture. The second, full 3D model, is superior in this sense – e.g., the forced convection heat transfer in the passages between the epoxy spacers. However, the extension of the 3D to the entire stator ensemble is too demanding for the usual, available computing resources.

As conclusive remarks, the numerical, FEM analysis complements the lumped-circuit approach. It gives valuable information on the paths that channel the heat from its source to the environment, and helps improving the thermal design of the HTS motor.

Acknowledgments

The authors acknowledge with gratitude the comments from Dr. P. Masson and Prof. C.A. Luongo and the support from the Office of Naval Research (ONR).

References

1. www.amsuper.com/products/index.cfm American Superconductor, May 2005
2. www.ecmweb.com/news/electric_siemens_first_operate/ Siemens, May 2005
3. Mellor, P., Roberts, D., and Turner, D. “Lumped parameter thermal model for electrical machines of TEFC

design", Proc. Inst. Elect. Eng., pt. B, vol. 138, no.5, Sept. 1991
4. Boglietti, A., Cavagnino, A., Lazzari, M., and Pastorelli, M., "A simplified thermal model for variable-speed self-cooled industrial induction motor", IEEE Trans. on Industrial Applications, 39, 4, pp. 945-952, 2003
5. Staton, D., Boglietti, A., and Cavagnino, A., "Solving the more difficult aspects of electric motor thermal analysis", www.cedrat.com/software/**motor**-cad/pdf/**motor**cad_IAS_2002_Digest.pdf
6. Postnikov, I.M., *Vibor optimalnih geometriceskih razmerov v elektriceskih mahinih*, Gosenergoizdat, Leningrad, 1952
7. MotorCad, *Thermal optimization of motors*, CEDRAT, www.cedrat.com
8. SPEED, *Thermal solver for electric motors*, www.elec.gla.ac.uk/groups/speed
9. Morega, Al.M., Ordonez, J.C. and Vargas, J.V.C, *Thermal model for the AC armature winding of a High Temperature Superconductor airborne motor*, ASME-IMECE Nov. 5-11, 2005, Orlando, Florida USA, accepted
10. FEMLAB, v.3.1*i*, Comsol, AB, www.comsol.com
11. Bejan, A. *Heat transfer*, NY, Wiley, 1993
12. Bejan, A. in *Heat Transfer Handbook*, Eds. Bejan, A. and Krauss, A.D., Ch.5 *Forced convection: Internal flows*, pp.395-438, J.Wiley, 2003.
13. Yovanovich, M.M., Culham, J.R. and Teertstra, P., "Calculating interface resistance", Electronics Cooling, www.electronics-cooling.com/Resources/EC_Articles/MAY97/article3.htm
14. DuPont Films – *High Performance Films KAPTON polyimide film*, Technical Information, Doc. H-54506-1 6/96 248387A (Replaces H-54506).